Phase diagram of the t-J model: A semiclassical calculation

W. Barford* and Jian Ping Lu†
The James Franck Institute and Department of Physics, The University of Chicago, 5640 South Ellis Avenue, Chicago, Illinois 60637

(Received 6 June 1990; revised manuscript received 23 August 1990)

The results of a semiclassical variational calculation of the t-J model are presented. The generalized staggered flux phases are introduced. It is found that these flux phases are stable for a large parameter range of the phase diagram. An interesting feature of these flux phases is that for small doping they have the best potential energy and for larger doping they have the best kinetic energy. It is also found that only those flux phases that do not break the local time reversal and parity symmetries are energetically favored. For sufficiently small J/t and doping the spiral phase is stable.

I. INTRODUCTION

The delicate competition between the holes in a doped quantum antiferromagnet to minimize their kinetic energy and for the spins to minimize their exchange energy is both a fascinating and difficult problem and one which is likely to lead to novel magnetic coherence. It has also been qualitatively argued[1] that the basic physics of the copper-oxide planes of the high-temperature superconductors may be described by the strongly correlated Hubbard model. For small doping this is equivalent to a model Hamiltonian which describes the motion of holes in an antiferromagnet, the so-called t-J model.[2] In this paper we present a semiclassical variational calculation which shows a rich phase diagram for this model.

We define the t-J Hamiltonian as

$$H = t \sum_{\langle ij \rangle} c_{i\sigma}^{\dagger} c_{j\sigma} + \text{H.c.} + J \sum_{\langle ij \rangle} (\mathbf{S}_i \cdot \mathbf{S}_j - \tfrac{1}{4} n_i n_j) , \qquad (1)$$

where $c_{i\sigma}^{\dagger}$ creates a fermion with spin σ on site i, $\mathbf{S}_i = \frac{1}{2} c_{i\sigma}^{\dagger} \boldsymbol{\sigma}_{\sigma\sigma'} c_{i\sigma'}$ and $n_i = c_{i\sigma}^{\dagger} c_{i\sigma}$ are spin and number operators, respectively, and $\langle ij \rangle$ represents nearest neighbors. (Throughout this paper the Einstein summation convention will be assumed for all Greek indices.) The Hamiltonian is understood to operate on empty or singly occupied states only. This Hamiltonian has been extensively studied. There is a wide body of evidence[3] from studies of the nonlinear σ model to exact diagonalizations and quantum Monte Carlo calculations which indicate that, at half-filling, there are long-range antiferromagnetic correlations. Experimentally, the undoped high-temperature superconductors show antiferromagnetic order.[4] However, there is much less concensus on the expected ground state as holes are doped.

By taking the continuum limit of this Hamiltonian, Shraiman and Siggia[5] found that, for small doping, the holes introduced a spiral distortion into the staggered magnetization. Kane *et al.*[6] came to a similar conclusion in a mean-field theory. Following Affleck and Marston, other mean-field theories have suggested the possibility of "flux phases" in which parity and time-reversal symmetries are either locally or globally broken.[7] However, one has to be cautious with $1/N$ mean-field theories as the Gutzwiller constraint is not correctly dealt with. Other studies have also suggested the stability of flux phases[8] for certain parameter ranges.

In an attempt to understand the phase diagram of this Hamiltonian by making well-controlled approximations, we construct variational wave functions which will provide rigorous upper bounds to the ground-state energy. We choose semiclassical wave functions, namely wave functions for which the spin orientation at each site is fixed and well defined, so quantum fluctuations are ignored. This enables us to strictly impose the Gutzwiller projection on the wave functions. Quantum fluctuations in the undoped quantum antiferromagnet merely renormalize the spin variables from that of the classical result.[3] Hence, for reasonably small doping, we expect that the neglect of quantum fluctuations will not qualitatively alter the phase diagram.

The plan of this paper is as follows: In the next section we derive an effective Hamiltonian which describes holes moving in a fixed spin background and present our variational procedure. We will show that the coupling of the holes to the spin background is equivalent to the motion of holes in a fictitious flux. Thus, in Sec. III we discuss the motion of spinless fermions in a generalized staggered flux. As we will see, certain flux arrangements can significantly lower the kinetic energy of the holes. The phase diagram within this scheme is presented in Sec. IV where we discuss the various phases. Finally, we conclude.

II. HOLES IN A STATIC SPIN BACKGROUND

A. The effective Hamiltonian

The Hamiltonian (1) acts only on the empty and singly occupied subspace. To take this constraint explicitly into account, we adopt the slave-fermion Schwinger-boson representation, which is to factorize the real electron operator

$$c_{i\sigma}^{\dagger} = f_i b_{i\sigma}^{\dagger} , \qquad (2)$$

where the $f_i^{\dagger}$ are fermion operators $\{f_i, f_j^{\dagger}\} = \delta_{ij}$, while the $b_{i\sigma}^{\dagger}$ are boson operators, $[b_{i\sigma}, b_{j\sigma'}^{\dagger}] = \delta_{ij}\delta_{\sigma\sigma'}$. The fermions and bosons necessarily satisfy the constraint

 ©1991 The American Physical Society

$b_{i\sigma}^\dagger b_{i\sigma}+f_i^\dagger f_i=1$ for each site. Notice that the representation (2) automatically projects out doubly occupied sites since

$$c_{i\sigma}^\dagger c_{i\sigma'}^\dagger = f_i f_i b_{i\sigma}^\dagger b_{i\sigma'}^\dagger \equiv 0 \ .$$

We may identify $f_i^\dagger$ as creating a hole on the ith site while $b_{i\sigma}^\dagger$ creates a spin. Substituting (2) into (1) the Hamiltonian now reads

$$H=-t\sum_{\langle ij\rangle}(f_j^\dagger f_i b_i^\dagger b_j+\text{H.c.}) + \frac{J}{4}\sum_{\langle ij\rangle}(1-n_i^f)(1-n_j^f)(b_i^\dagger \boldsymbol{\sigma} b_i \cdot b_j^\dagger \boldsymbol{\sigma} b_j - 1) \ , \quad (3)$$

where $\boldsymbol{\sigma}$ is the Pauli spin matrix, $n_i^f=f_i^\dagger f_i$ is the fermion number operator, and we have introduced the spinor notation for the bosons

$$b_i=\begin{bmatrix} b_{i\uparrow} \\ b_{i\downarrow} \end{bmatrix} \ .$$

It is clear from (3) that the spinless fermions and spinney bosons are intimately coupled. Ideally one would like to diagonalize this Hamiltonian for both the hole and spin degrees of freedom. Since we cannot do this it is necessary to make some simplifying assumptions. Our assumption is that, in the presence of strong antiferromagnetic correlations, the key physics is that the hole movement is renormalized due to its coupling to the spin background. We will take a semiclassical approximation and assume that the spin degrees of freedom are frozen and study the consequences of particular spin configurations on the hole dynamics. (On the other hand, to investigate the spin dynamics the hole background may be fixed.) The spin background will be taken as variational parameters.

We wish to show that the Hamiltonian (3) diagonalized in a Hilbert space of fixed spin orientations is equivalent to an effective Hamiltonian in which there are only hole degrees of freedom. Let the fixed spin background through which the holes hop be denoted by

$$|\psi_s\rangle=\prod_{i=1}^{N} b_{i\uparrow}^\dagger(\hat{\mathbf{z}}_i)|0\rangle \ , \quad (4)$$

where $b_{i\uparrow}^\dagger(\hat{\mathbf{z}}_i)$ creates an up spin on the ith site quantized along the direction $\hat{\mathbf{z}}_i$. $\hat{\mathbf{z}}_i$ is denoted by the Euler angles ϕ_i and θ_i (i.e., the azimuthal and polar angles) with respect to the global axis of quantization $\hat{\mathbf{z}}$. In terms of the global axis of quantization we may write

$$|\Omega_i\rangle=b_{i\uparrow}^\dagger(\hat{\mathbf{z}}_i)|0\rangle=\begin{bmatrix} \cos\left[\frac{\theta_i}{2}\right] \\ e^{i\phi_i}\sin\left[\frac{\theta_i}{2}\right] \end{bmatrix} \quad (5)$$

in the coherent state representation.

Holes are created by annihilating spins; for a single doped hole the ith basis state is

$$|i\rangle=f_i^\dagger b_{i\uparrow}(\hat{\mathbf{z}}_i)|\psi_s\rangle \ . \quad (6)$$

In general, for n doped holes, the basis states are of the form

$$|[i,j,k,\ldots]\rangle = [f_i^\dagger f_j^\dagger f_k^\dagger \cdots][b_{i\uparrow}(\hat{\mathbf{z}}_i)b_{j\uparrow}(\hat{\mathbf{z}}_j)b_{k\uparrow}(\hat{\mathbf{z}}_k)\cdots]|\psi_s\rangle \ , \quad (7)$$

where there are n terms within the square brackets.

The matrix elements of H within the subspace are readily calculable. Consider first the H_{KE} and only one hole; the representative basis state is denoted by $|i\rangle$ (6). Then the action of the hopping part of the Hamiltonian on this state will be to hop the hole from site i to a neighboring site j and transport the spin on the jth site coherently to site i:

$$H_{\text{KE}}|i\rangle=-tf_j^\dagger f_i b_{i\sigma}^\dagger b_{j\sigma} f_i^\dagger b_{i\uparrow}(\hat{\mathbf{z}}_i)|\psi_s\rangle = -tf_j^\dagger b_{j\uparrow}(\hat{\mathbf{z}}_i)|\psi_s\rangle \ .$$

Within the fixed spin configuration subspace the only nonzero overlap is with the basis state $|j\rangle$ and it is

$$H_{ji}^{\text{KE}}=\langle j|H_{\text{KE}}|i\rangle = -t\langle\psi_s|f_j b_{j\uparrow}^\dagger(\hat{\mathbf{z}}_j)b_{j\uparrow}(\hat{\mathbf{z}}_i)f_j^\dagger|\psi_s\rangle = -t\langle\Omega_i|\Omega_j\rangle \ , \quad (8)$$

which is a product of the orbital wave-function overlap and spin wave-function overlap.

Using (5) it is easily shown that[9]

$$t_{ji}\equiv t\langle\Omega_i|\Omega_j\rangle = t[\cos(\theta_i/2)\cos(\theta_j/2)+e^{i(\phi_j-\phi_i)}\sin(\theta_i/2)\sin(\theta_j/2)] = t[\tfrac{1}{2}(1+\hat{\boldsymbol{\Omega}}_i\cdot\hat{\boldsymbol{\Omega}}_j)]^{1/2}e^{(i/2)\hat{\omega}(\hat{\boldsymbol{\Omega}}_i,\hat{\boldsymbol{\Omega}}_j;\hat{\mathbf{z}})} \ , \quad (9)$$

where $\hat{\boldsymbol{\Omega}}_i=(\sin\theta_i\cos\phi_i,\sin\theta_i,\sin\phi_i,\cos\theta_i)$ is the unit vector along the local axis of quantization $\hat{\mathbf{z}}_i$ for the ith spin. Evidently the magnitude of the hopping amplitude is reduced by a factor depending on $\hat{\boldsymbol{\Omega}}_i\cdot\hat{\boldsymbol{\Omega}}_j$ while the phase is proportional to $\hat{\omega}$, the solid angle subtended by the two spins and the global axis of quantization. This phase is manifestly ambiguous as the global axis of quantization is arbitrary—this corresponds to a gauge degree of freedom. The invariant quantity is the solid angle spanned by the four spins surrounding a plaquette which corresponds to twice the fictitious flux threading the plaquette.

In a similar manner we may calculate the matrix element of H_{PE} between any two basis states. This will only give a diagonal contribution. For example, if $|i,j\rangle$ represents a basis state in which there are only spins on sites i and j then

$$\langle i,j|H_{\text{PE}}|i,j\rangle=\tfrac{1}{4}(\hat{\boldsymbol{\Omega}}_i\cdot\hat{\boldsymbol{\Omega}}_j-1) \ . \quad (10)$$

Consequently, we may introduce an effective Hamiltonian in which the spin degrees of freedom are taken to be classical,

$$H_{\text{eff}} = -\sum_{\langle ij \rangle} (t_{ij} f_i^\dagger f_j + \text{H.c.}) + \frac{J}{4} \sum_{\langle ij \rangle} (1-n_i^f)(1-n_j^f)(\hat{\Omega}_i \cdot \hat{\Omega}_j - 1) , \quad (11)$$

and where the Hilbert space is spanned by the hole basis states of the form

$$|i,j,k,\ldots\rangle = f_i^\dagger f_j^\dagger f_k^\dagger \cdots |0\rangle . \quad (12)$$

From the effective Hamiltonian it may be observed that the spin background affects the hole motion in two ways. Firstly, it introduces an effective attractive interaction between two holes on neighboring sites: this may serve as a possible pairing mechanism for holes. Secondly, an almost antiferromagnetically correlated spin background dramatically reduces the hole-hopping amplitude ($|t_{ij}| < t$). There is therefore a tendency for the spins to distort away from being antiferromagnetically aligned when the doping is increased—this is just the Nagaoka[10] tendency to drive the spins ferromagnetic. Furthermore, the hopping amplitude of the holes may be chosen to be complex and hence a spin configuration can be constructed which mimics a fictitious flux. We will show presently that such spin configurations can significantly lower the kinetic energy of the holes. It is this competition between the kinetic energy and exchange energy which gives rise to the richness and the complexity of the problem.

B. The variational wave function

Even though the spin degrees of freedom have been frozen, we are still left with the formidable problem of solving (11). Our approach will be to construct a variational wave function which will be an eigenstate of H_{KE} only, and then calculate the expectation value of H_{PE}. Provided that the $\{t_{ij}\}$ are chosen so that there is translational symmetry, H_{KE} can be trivially Bloch diagonalized and its ground-state wave function $|\tilde{\psi}\rangle$ is formed by filling up the Bloch states $|f_{\mathbf{k},n}\rangle$ of energy $\varepsilon_{\mathbf{k},n}$ to the Fermi level ε_f (n is a band index),

$$|\tilde{\psi}\rangle = \prod_{\varepsilon_{\mathbf{k},n} < \varepsilon_f} f_{\mathbf{k},n}^\dagger |0\rangle . \quad (13)$$

We can calculate the expectation value of the energy,

$$\langle E(\{\theta_i,\phi_i\})\rangle = \langle \tilde{\psi}(\{\theta_i,\phi_i\}) | H_{\text{eff}} | \tilde{\psi}(\{\theta_i,\phi_i\})\rangle . \quad (14)$$

The kinetic part is the sum of the spinless fermion spectrum up to the Fermi energy

$$\langle E_{\text{KE}} \rangle = \sum_{\varepsilon_{\mathbf{k},n} < \varepsilon_f} \varepsilon_{\mathbf{k},n} , \quad (15)$$

while the exchange energy is

$$\langle E_{\text{PE}} \rangle = \frac{J}{4} \sum_{\langle ij \rangle} \langle (1-n_i^f)(1-n_j^f)\rangle (\hat{\Omega}_i \cdot \hat{\Omega}_j - 1) . \quad (16)$$

Given the Bloch wave function (13), the expectation value of the particle-particle correlation function can be calculated. Its derivation and resulting expression are shown in the Appendix.

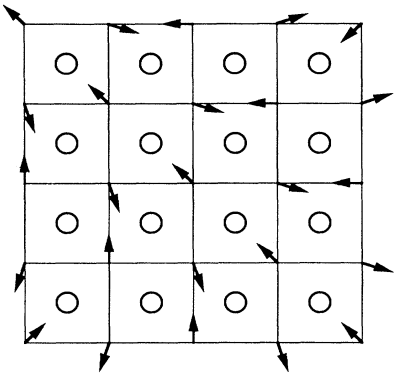

FIG. 1. An example of the (1,1) spiral phase. Arrows indicate the local spin direction projected onto the x-z plane. All spins have the same azimuthal angle and therefore the flux through every plaquette is zero. The z axis is out of the paper.

We now have a prescription for calculating the expectation value of the energy for a given spin configuration which is to be minimized with respect to $\{\theta_i,\phi_i\}$; all that remains is for us to construct some suitable spin configurations. We consider two broad classes of spin configurations.

(i) Fluxless phase configurations. In this case t_{ij} may be complex but $\prod_{i,j} t_{ij}$ around a plaquette is real, thus the holes have a tight-binding spectrum. Spiral and canting configurations fall into this class. Figure 1 shows the spin configuration for a (1,1) spiral phase. Let θ_{ij} be the angle between two neighboring spins, viz.,

$$\theta_{ij} = \cos^{-1}(\hat{\Omega}_i \cdot \hat{\Omega}_j) , \quad (17)$$

then from (9)

$$|t_{ij}| = t \cos\left[\frac{\theta_{ij}}{2}\right] . \quad (18)$$

(ii) Flux phase configurations. In general,

$$\prod_{i,j} t_{ij} = \prod_{i,j} |t_{ij}| e^{i\Phi} ,$$

where we may interpret Φ as the fictitious flux which couples to the holes and, from above, is half the solid angle subtended by the four spins surrounding the plaquette.

Of the possible spin configurations, the flux phase is of particular interest and has been extensively studied in both a mean-field approach[7] and Monte Carlo simulations.[8] But why should they be relevant? One clue comes from the interesting work of Hasegawa and co-workers[11] who showed that the kinetic energy of spinless fermions in a uniform magnetic field is an absolute minimum when there is one flux quantum per particle. This is the so-called commensurate flux phase (CFP). This suggests the possibility that, in spin configurations which mimic a flux, the kinetic energy of the holes is lowered. However, a CFP cannot be constructed from a fixed spin back-

ground near the Néel state because the CFP breaks the global time-reversal (T) symmetry. In contrast, the time-reversal symmetry is only broken locally in the Néel state and it may be restored by a lattice translation (R). This suggests that the staggered flux phase (SFP), which has an alternating flux through nearest-neighbor plaquettes, will be more relevant for our problem. Indeed, such a phase can be constructed.

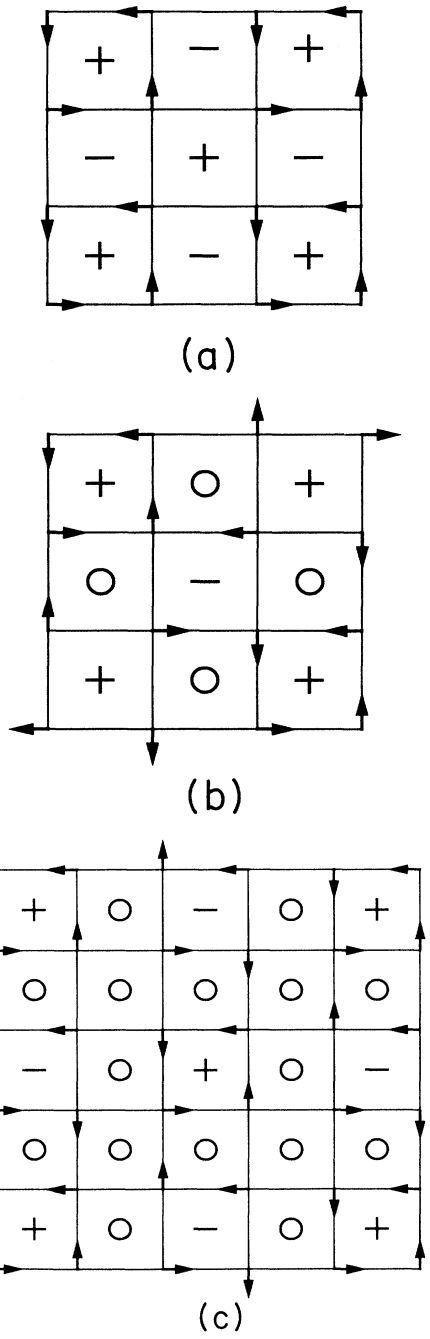

FIG. 2. The spin configurations corresponding to (a) the $q=2$, (b) the $q=4$, and (c) the $q=8$ flux phases. In all cases arrows indicate the projection of the spins onto the x-y plane. The spins on the A and B sublattices have polar angles α and β, respectively. + and − represent the polarity of the flux threading the plane and z points out of the paper.

Consider the spin configuration shown in Fig. 2(a). The azimuthal angles of neighboring spins differ by $\pi/2$. If the polar angles are α and β for spins on the A and B sublattices, respectively, then the solid angle subtended by the four spins around a plaquette is

$$\hat{\omega}=8\tan^{-1}[\tan(\alpha/2)\tan(\beta/2)] \tag{19}$$

and the fictitious flux threading the plaquette is $\Phi=\hat{\omega}/2$. If $\beta=\pi-\alpha$ then $\Phi=\pi(-1)^r$ and we form the π staggered flux phase. In this paper we will take $\beta=\pi-\alpha$ if the relative angle θ (17) is $\geq\pi/2$ and $\beta=\alpha$ if θ is $<\pi/2$.

In constructing various spin configurations as candidates to minimize the energy of the Hamiltonian (3), we are naturally led to the concept of the generalized staggered flux phase (GSFP) for which the translation operator R, which restores time-reversal invariance, is not restricted to a nearest-neighbor lattice vector, but is a finite lattice translation vector

$$R=[x\rightarrow x+m, y\rightarrow y+n] .$$

As we will see, this gives rise to a variety of flux phases which become important for small doping.

Since, as we have said, the variational wave functions are eigenstates of the kinetic energy, we obtain useful insight about the structure of the phase diagram by considering this term alone. In the next section we will therefore study the problem of spinless fermions moving in a generalized staggered flux.

III. SPINLESS FERMIONS IN A GENERALIZED STAGGERED FLUX

The Hamiltonian which describes the motion of spinless fermions in a staggered flux can be written as

$$H_{\rm KE}=-\sum_{\langle ij\rangle} e^{i\phi_{ij}} f_i^\dagger f_j+\text{H.c.} , \tag{20}$$

where ϕ_{ij} is the gauge potential on the link ij. It is important to notice that, although the definition of ϕ_{ij} depends on the particular gauge, the physically relevant quantity is the gauge invariant flux Φ through a plaquette p

$$\Phi_p=\sum_{\langle ij\rangle\subset p}\phi_{ij} . \tag{21}$$

We consider flux arrangements for which the magnetic unit cell contains q plaquettes but where only two are pierced with alternating flux of magnitude Φ_p. The average flux magnitude per unit cell $\Phi_{\rm av}$ is then $2|\Phi_p|/q$. Among the various flux patterns examined, we found that the ones with the highest symmetry have the lowest kinetic energy. We denote these as generalized staggered flux phases. The well-known example is the $q=2$ case shown in Fig. 2(a), the $q=4$ and 8 examples are shown in Figs. 2(b) and 2(c).

Table I shows the kinetic energy per site for various dopings as a function of q when $|\Phi_p|$ is π so that

TABLE I. The kinetic energy per site for spinless fermions in the q generalized π staggered flux for filling x with various values of q.

x	$\frac{1}{q}$	0	$\frac{1}{32}$	$\frac{1}{16}$	$\frac{1}{8}$	$\frac{1}{4}$	$\frac{1}{2}$
$\frac{1}{32}$		−0.118 956	−0.117 320	−0.112 216	−0.104 996	−0.088 378	−0.086 227
$\frac{1}{16}$		−0.226 264	−0.223 518	−0.221 948	−0.207 129	−0.176 650	−0.168 393
$\frac{1}{8}$		−0.408 076	−0.404 783	−0.402 156	−0.401 658	−0.351 971	−0.321 258
$\frac{1}{4}$		−0.656 427	−0.656 250	−0.652 540	−0.652 075	−0.677 473	−0.589 499
$\frac{1}{2}$		−0.810 755	−0.817 117	−0.820 120	−0.831 108	−0.833 707	−0.958 092

$\Phi_{\text{av}}=2\pi/q$. We observe that, for hole dopings of less than $\frac{1}{8}$, the tight binding (zero flux) phase has the best energy whereas for hole doping of greater than $\frac{1}{8}$, a flux phase always has better energy. Indeed, for the latter case, given a doping x, the best kinetic energy occurs when Φ_{av} is commensurate with the doping. For example, at a doping of one-quarter, the best kinetic energy occurs for the $q=4$ flux phase which has an energy of -0.6675 versus -0.6562 for the tight-binding case. The density of states for the $q=2$ case is shown in Fig. 3(a). There are two bands which are degenerate at $E=0$. The $q=4$ density of states is shown in Fig. 3(b); here there are four bands. Notice that this problem bears a resemblance to the uniform flux problem in so far that the best kinetic energy of the holes at a quarter filling is the $q=4$ phase where the lowest band is filled and for one-half filling, the $q=2$ phase is best with the lower band full. However, there are no gaps between the bands as in the uniform flux problem[12] and, unlike that problem, there is no flux pattern which can lower the kinetic energy for sufficiently small doping. Figure 4 shows the kinetic energy per site for the tight binding $q=4$ and 2 cases as a function of doping when $|\Phi_p|=\pi$. For $0.23\le x\le 0.39$ and $0.61\le x\le 0.77$, the $q=4$ phase has the lowest kinetic energy while for $0.39\le x\le 0.61$, the $q=2$ phase is lowest. If Φ_p is decreased from π then the energy differences between the flux phases and tight binding monotonically decrease to zero as illustrated in Fig. 5.

Finally, we should observe that, in general, the Hamiltonian (20) breaks local parity and time-reversal symmetries which may be restored under a suitable lattice translation, however, if $\Phi_p=\pi$, then local parity and time-reversal symmetries are not broken.[13] Indeed, the current of spinless fermions around each plaquette, defined as

$$\mathcal{J}_{ij}^{\text{hole}}=-i\langle e^{i\phi_{ij}}f_i^\dagger f_j-e^{i\phi_{ji}}f_j^\dagger f_i\rangle\ , \tag{22}$$

is found to be precisely zero. This has important implications in the next section [see (32)].

Since for sufficiently high doping the $q=2$ and 4 GSFP have lower kinetic energy than the tight-binding spectrum, we may anticipate the next section by stating that spin configurations which correspond to such flux phases are good candidates to minimize the total energy for certain parameter ranges.

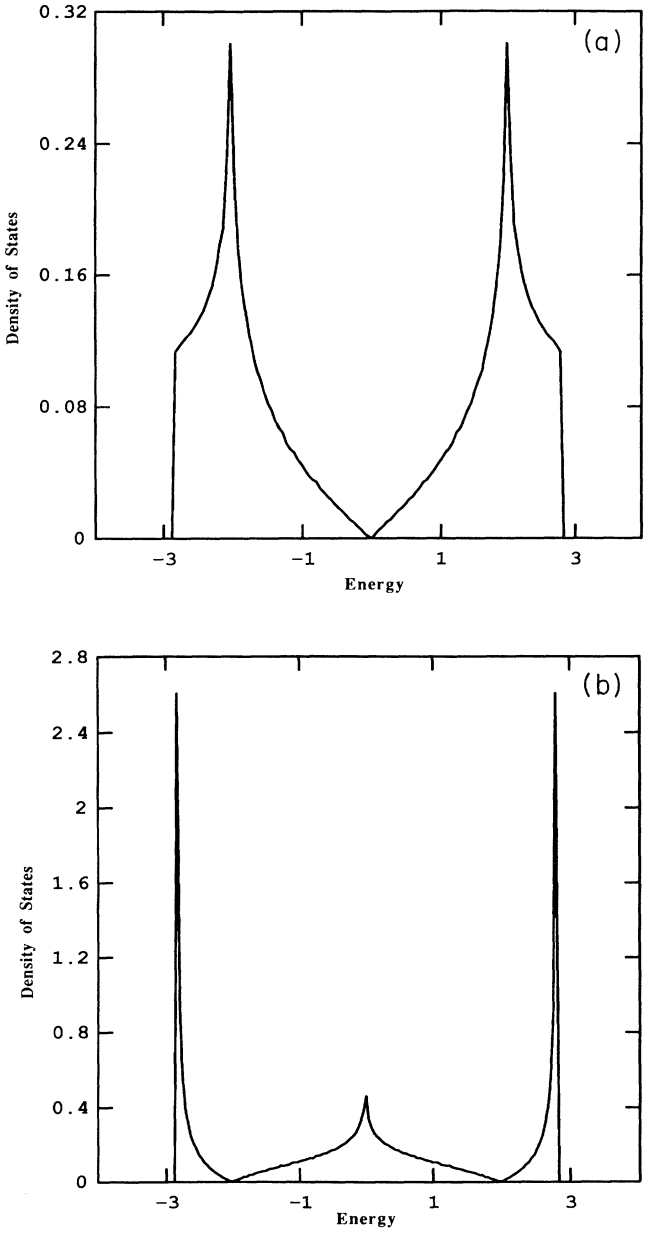

FIG. 3. (a) Density of states for the $q=2$ π flux phase. (b) The same for $q=4$.

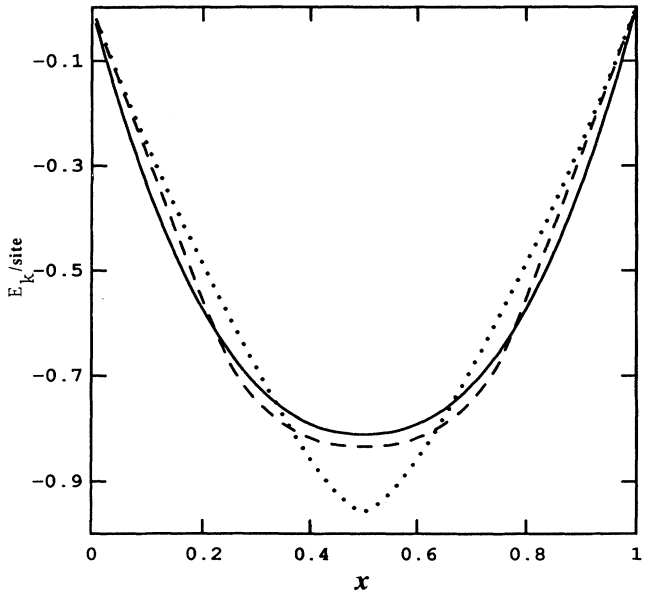

FIG. 4. Kinetic energy per site as a function of doping when $\Phi_p=\pi$. The solid curve is for zero flux and the dashed and dotted curves are for the $q=4$ and 2 π flux phases, respectively.

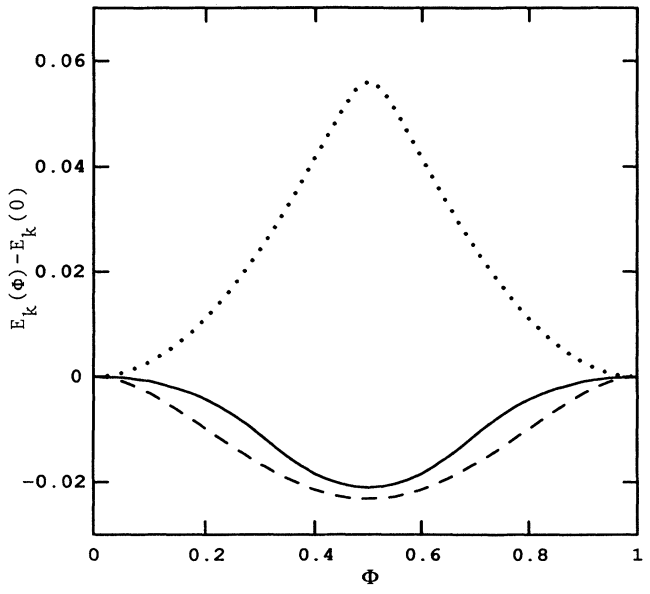

FIG. 5. The difference in kinetic energy per site between the $q=4$ flux phase and tight binding at one-eighth (dotted), one-quarter (solid), and one-half (dashed) filling as a function of $|\Phi_p|/2\pi$.

IV. THE PHASE DIAGRAM

In this section we calculate the expectation value of the Hamiltonian (11) at a given doping

$$x=\frac{1}{N}\sum_{\varepsilon_{\mathbf{k},n}<\varepsilon_f(x)}1$$

for the various spin configurations considered in Secs. II and III. Using Eqs. (15)–(18), the total energy per site as a function of the angle θ between two neighboring spins can be written as

$$\varepsilon(\theta)=t\eta(x)\cos(\theta/2)+\frac{J}{2}\rho(x)\cos\theta\ , \tag{23}$$

where

$$\eta(x)=\frac{1}{N}\sum_{\tilde{\varepsilon}_{\mathbf{k},n}<\tilde{\varepsilon}_f(x)}\tilde{\varepsilon}_{\mathbf{k},n} \tag{24}$$

and

$$\rho(x)=\langle(1-n_i^f)(1-n_j^f)\rangle\ . \tag{25}$$

The average in (25) is taken over the ground state of the Hamiltonian (20), and $\tilde{\varepsilon}_{\mathbf{k},n}$ in (24) is its spectrum. The explicit calculation for ρ is given in the Appendix. For the spiral, canting, and π flux phases, η and ρ are independent of θ.[14] Minimizing $\varepsilon(\theta)$ with respect to θ gives

$$\frac{\partial\varepsilon}{\partial\theta}=-\sin(\theta/2)\left[\frac{t}{2}\eta+J\rho\cos\left[\frac{\theta}{2}\right]\right]\ , \tag{26}$$

whence

$$\theta_{\rm eq}(x)=2\cos^{-1}\left[-\frac{t\eta(x)}{J\rho(x)}\right] \tag{27}$$

and

$$\varepsilon_{\rm eq}(x)=-\frac{\eta^2(x)t^2}{4J\rho(x)}-\frac{J\rho(x)}{2} \tag{28}$$

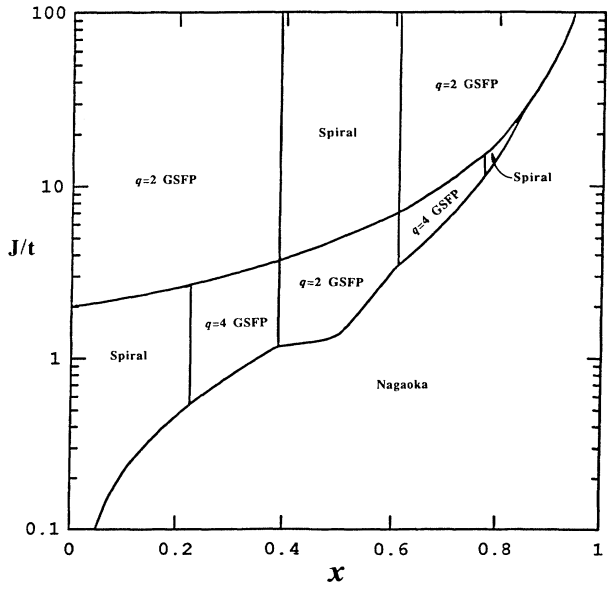

FIG. 6. The phase diagram for the t-J model.

upon setting (26) to zero.

The phases with the lowest energy are shown in Fig. 6. There are four competing phases: (1) spiral, (2) $q=4$ flux phase, (3) $q=2$ flux phase, and (4) the Nagaoka ferromagnet. The Nagaoka ferromagnet is stable when the kinetic energy of the holes completely dominates, this occurs for $J/t<(J/t)_c$, where $(J/t)_c$ progressively increases as the doping increases. When J/t is large, θ_{eq} is close to π, the hole-hopping amplitude is strongly renormalized, and the Heisenberg energy dominates. We find that, for $0\leq x\leq 0.39$ and $0.71\leq x\leq 1$, the $q=2$ flux phase has the best energy whereas for intermediate doping, the spiral phase is stable. This result coincides with previous studies which showed that flux phases were stable for small doping at large J/t.[8] For intermediate values of J/t [namely $O(1)$], the kinetic energy of the holes becomes important in determining the magnetic coherence especially for large doping. We find that, as the doping is increased, there is a phase transition from a spiral to a $q=4$ phase at $x\sim 0.23$, and at $x\sim 0.39$ the $q=2$ phase is entered. As the doping is further increased, there is a reversal of this trend. This may be easily understood from the analysis of the last section which showed that, for hole dopings between 0.23 and 0.77, a flux phase always has better kinetic energy than a fluxless phase.

Let us now examine how θ_{eq} behaves as a function of doping and J/t. When the doping is small $\eta\simeq -4x$ and $\rho\simeq(1-x)^2$, then from (27) the distortion away from Néel order is

$$\tilde{\theta}_{eq}=\pi-\theta_{eq}\simeq\frac{4tx}{J(1-x)^2}\ . \tag{29}$$

This rederives the results of Shraiman and Siggia.[5] Notice that the only important quantity is the relative angle between neighboring spins and therefore there is no distinction between canting and spiral phases, for example. Including quantum fluctuations will favor the spiral distortion.[6] We can see that, in order to minimize their kinetic energy, doped holes introduce a long-range spiral or canting distortion in the Néel background.

The Nagaoka limit can also be found from (27) for small doping; this is defined as the limit that $\theta_{eq}\to 0$ or

$$\frac{2tx}{J(1-x)^2}\geq 1 \tag{30}$$

implying that

$$\left[\frac{J}{t}\right]_c=\frac{2x}{(1-x)^2}\ . \tag{31}$$

Turning to the more quantitative results, in Fig. 7(a), we plot θ_{eq} versus x for three values of J/t: 0.5, 1.5, and 30. $J/t=0.5$ corresponds to a cut through the spiral phase to the Nagaoka state. As expected, θ_{eq} decreases as the doping is increased. $J/t=30$ cuts through the $q=2$ flux phase, spiral phase, back to the $q=2$ flux phase, and finally to the Nagaoka phase. θ_{eqa} decreases smoothly but more slowly as a function of x until it reaches $\pi/2$ whereupon it jumps to zero. The third plot for $J/t=1.5$ is very interesting. Here we cut through the spiral to the $q=4$ and then to the $q=2$ phase. Initially θ_{eq} decreases smoothly, however, notice that θ_{eq} plateaus at $\pi/2$ in the flux phases for x between 0.36 and 0.51. At $x=0.51$, θ_{eq} discontinuously falls to zero.

Similar features are shown in Fig. 7(b) for θ_{eq} as a function of J/t at $x=\frac{1}{8}$, $\frac{1}{4}$, and $\frac{1}{2}$. $x=\frac{1}{8}$ cuts through the $q=2$ flux and spiral phases; aside from the small discontinuity at the phase boundary, θ_{eq} varies smoothly to zero. However, for $x=\frac{1}{4}$ and $\frac{1}{2}$, when J/t is small, the cuts pass through the $q=4$ and 2 flux phases, respective-

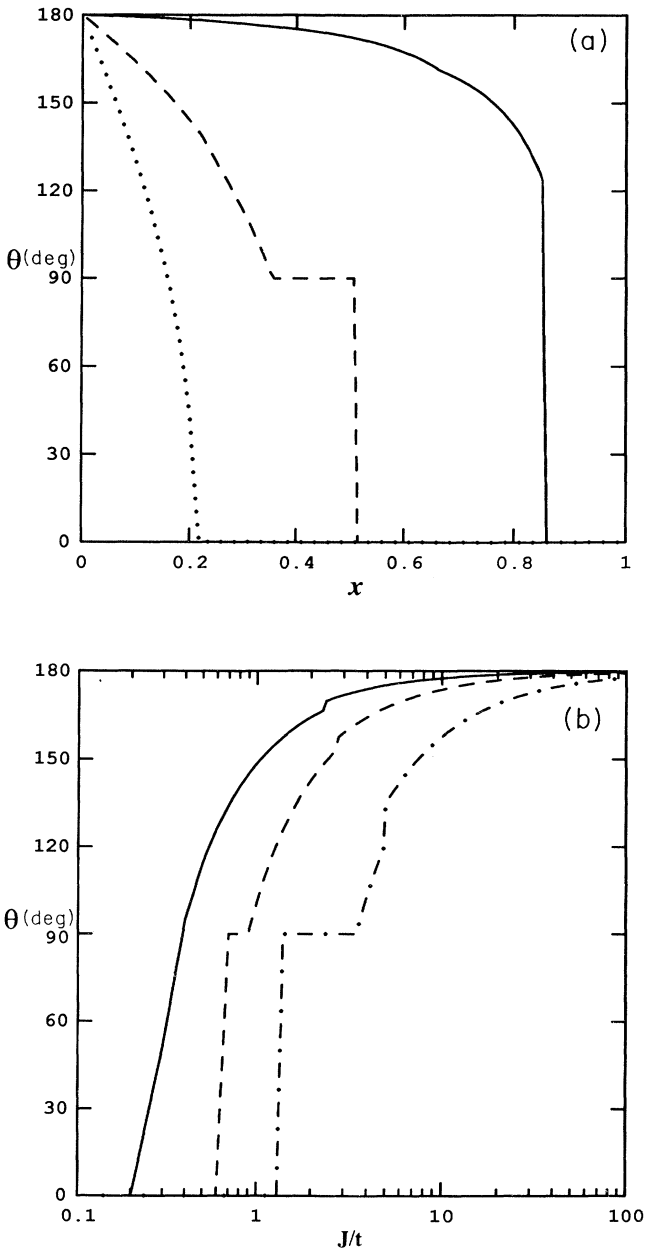

FIG. 7. (a) θ_{eq} vs hole doping (x) for $J/t=0.5$ (dotted), 1.5 (dashed), and 30 (solid). (b) θ_{eq} vs J/t for dopings of $\frac{1}{8}$ (solid), $\frac{1}{4}$ (dashed), and $\frac{1}{2}$ (dotted).

ly. Once again there are plateaus over a significant parameter range where θ_{eq} remains at $\pi/2$ before jumping to zero.

At first sight these plateaus seem rather surprising. Naively one would argue that as J/t is lowered, the kinetic energy becomes more important and so θ_{eq} decreases. The hole-hopping amplitude therefore increases with no discontinuous behavior at $\pi/2$. However, for the flux phases we must remember that, when $\theta_{eq} \geq \pi/2$, the polar angles of the spins on the sublattices A and B are α and $\beta=\pi-\alpha$, respectively, so the flux through a plaquette is always π. But when $\theta_{eq} < \pi/2$, we have $\alpha=\beta$ so the flux is less than π (19). Hence, η [defined in (24)] increases with decreasing θ_{eq} and so the gain in kinetic energy cannot compete with the loss of the potential energy. This accounts for the remarkable stability of the $\theta_{eq}=\pi/2$ plateau. There is a significant consequence associated with this plateau, namely that the flux through a plaquette Φ_p is always π. We thus come to an important conclusion that the "flux" phases are stable only if the local P and T symmetries are not broken. As a result the current of electrons around a plaquette

$$\begin{aligned}\mathcal{J}_{ij}^{\text{phys}} &= i\langle c_{i\sigma}^{\dagger}c_{j\sigma} - c_{j\sigma}^{\dagger}c_{i\sigma}\rangle \\ &= i\langle e^{i\phi_{ij}}f_i^{\dagger}f_j - e^{i\phi_{ji}}f_j^{\dagger}f_i\rangle \\ &= -\mathcal{J}_{ij}^{\text{hole}} \end{aligned} \tag{32}$$

is always zero. These results suggest that the ground state of the t-J Hamiltonian does not break local P and T symmetries.

V. CONCLUSIONS

In this paper we presented a variational calculation of the phase diagram of the t-J model within the semiclassical approximation. Generalized staggered flux phases were introduced. We found that these flux phases are stable for a large parameter range. This can be understood by considering the essential physics: for small doping the Heisenberg term dominates while for larger doping it is the kinetic energy which is important. The remarkable feature of the GSFP is that, for small doping, they have the best potential energy and for larger doping they have the best kinetic energy. Indeed, there is a window of J/t for which the GSFP is stable over a large range of doping. For sufficiently small J/t and doping, we found that the spiral phase is stable, in agreement with earlier work.[5,6] Another important result is that only those GSFP states which *do not* break the local time-reversal and parity symmetries are energetically favored. This appears to be consistent with most of the experimental measurements on time-reversal symmetry breaking in the high-T_c materials.[15]

In our analysis we have neglected quantum fluctuations. It is expected that, at a certain doping, the spins will become disordered but on short length scales they would still remain correlated. The semiclassical variational calculation will therefore encapsulate the key physics of the competition between the kinetic energy of the holes and the potential energy of the spins. We have shown, by taking the Gutzwiller projection explicitly into account, that at $x \sim \frac{1}{4}$ and $J/t \sim O(1)$, the novel flux phases are stable because the fictitious flux, generated by the spins, can significantly reduce the kinetic energy of the holes. We expect that the introduction of quantum fluctuations will not alter this result. However, for sufficiently large doping, the picture of holes moving through a spin background becomes invalid. We would then expect that the phase diagram is no longer qualitatively correct. Indeed, it is known that when $x > 0.864$, the Nagaoka ferromagnet is not stable.[16]

ACKNOWLEDGMENTS

We would like to thank Dr. J. H. Kim, Professor K. Levin, Dr. S. Liang, Dr. J. Marko and Mr. Q. Si for helpful discussions and comments. This work was supported by the National Science Foundation–Science and Technology Center for Superconductivity (NSF-STC) Grant No. NSF-STC-8809854.

APPENDIX

It is the purpose of this appendix to derive an expression for the expectation value of the nearest-neighbor particle-particle correlation function. That is, we require

$$\begin{aligned}\rho &= \langle\tilde{\psi}|(1-f_i^{\dagger}f_i)(1-f_j^{\dagger}f_j)|\tilde{\psi}\rangle \\ &= 1-\langle\tilde{\psi}|f_i^{\dagger}f_i|\tilde{\psi}\rangle - \langle\tilde{\psi}|f_j^{\dagger}f_j|\tilde{\psi}\rangle \\ &\quad + \langle\tilde{\psi}|f_i^{\dagger}f_if_j^{\dagger}f_j|\tilde{\psi}\rangle\ , \end{aligned} \tag{A1}$$

where $|\tilde{\psi}\rangle$ is constructed by filling up all the allowed states to the Fermi energy:

$$|\tilde{\psi}\rangle = \prod_{\varepsilon_{\mathbf{k},n}<\varepsilon_f} f_{\mathbf{k}n}^{\dagger}|0\rangle\ . \tag{A2}$$

Here $f_{\mathbf{k}n}^{\dagger}$ creates a quasiparticle with crystal momentum $\mathbf{k}$ in the nth band.

Generally it will be necessary to consider more than one atom per unit cell. Let $f_{\gamma i}^{\dagger}$ create a spinless fermion on the ith atom of the γth unit cell. If $f_{\mathbf{k}i}^{\dagger}$ is the Fourier transform of $f_{\gamma i}^{\dagger}$, namely,

$$f_{\mathbf{k}i}^{\dagger} = \frac{1}{\sqrt{N}}\sum_{\text{unit cells}} e^{i\mathbf{k}\cdot\mathbf{R}_i}f_{\gamma i}^{\dagger} \tag{A3a}$$

so that

$$f_{\gamma i}^{\dagger} = \frac{1}{\sqrt{N}}\sum_{\mathbf{k}} e^{-i\mathbf{k}\cdot\mathbf{R}_i}f_{\mathbf{k}i}^{\dagger}\ , \tag{A3b}$$

then the quasiparticle creation operator is

$$f_{\mathbf{k}n}^{\dagger} = \alpha_{ni}(\mathbf{k})f_{\mathbf{k}i}^{\dagger} \tag{A4a}$$

and the inverse relation is

$$f_{\mathbf{k}i}^{\dagger} = \beta_{in}(\mathbf{k})f_{\mathbf{k}n}^{\dagger}\ , \tag{A4b}$$

where $\underline{\beta}=\underline{\alpha}^{-1}$.

Let us first calculate $\langle\tilde{\psi}|f_i^{\dagger}f_i|\tilde{\psi}\rangle = \langle n_i^f\rangle$. This is

$$\left\langle 0 \left| \prod_{\mathbf{k},n} f_{\mathbf{k}n} \frac{1}{N} \sum_{k_1,k_2,n_1,n_2} \beta_{in_1}(\mathbf{k}_1)\beta^*_{in_2}(\mathbf{k}_2) f^\dagger_{k_1 n_1} f_{k_2 n_2} e^{i(\mathbf{k}_1-\mathbf{k}_2)\cdot\mathbf{R}_i} \prod_{\mathbf{k},n} f^\dagger_{\mathbf{k}n} \right| 0 \right\rangle$$

upon substituting Eqs. (A2), (A3b), and (A4b). This is identically zero unless $\{\mathbf{k}_1,n_1\}=\{\mathbf{k}_2,n_2\}<\varepsilon_f$ whereupon

$$\langle n_i^f \rangle = \frac{1}{N} \sum_{\mathbf{k},n<\varepsilon_f} \beta_{in}(\mathbf{k})\beta^*_{in}(\mathbf{k}) \ . \tag{A5}$$

The two-site correlation function $\langle \tilde{\psi}|f_i^\dagger f_i f_j^\dagger f_j|\tilde{\psi}\rangle = \langle n_i^f n_j^f \rangle$ is

$$\left\langle \tilde{\psi} \left| \frac{1}{N^2} \sum_{k_1,k_1',k_2,k_2',n_1,n_1',n_2,n_2'} \beta_{in_1}(\mathbf{k}_1)\beta^*_{in_1'}(\mathbf{k}_1')\beta_{jn_2}(\mathbf{k}_2)\beta^*_{jn_2'}(\mathbf{k}_2') f^\dagger_{k_1 n_1} f_{k_1' n_1'} f^\dagger_{k_2 n_2} f_{k_2' n_2'} e^{i(\mathbf{k}_1-\mathbf{k}_1')\cdot\mathbf{R}_i} e^{i(\mathbf{k}_2-\mathbf{k}_2')\cdot\mathbf{R}_j} \right| \tilde{\psi} \right\rangle \ .$$

Unless either (i) $\{\mathbf{k}_1,n_1\}=\{\mathbf{k}_1',n_1'\}$ and $\{\mathbf{k}_2,n_2\}=\{\mathbf{k}_2',n_2'\}$ or (ii) $\{\mathbf{k}_1,n_1\}=\{\mathbf{k}_2',n_2'\}$ and $\{\mathbf{k}_2,n_2\}=\{\mathbf{k}_1',n_1'\}$, this term is also identically zero. Considering (i) first, we have

$$\frac{1}{N^2} \sum_{\mathbf{k}_1,n_1<\varepsilon_f} \beta_{in_1}(\mathbf{k}_1)\beta^*_{in_1}(\mathbf{k}_1) \sum_{\mathbf{k}_2,n_2<\varepsilon_f} \beta_{jn_2}(\mathbf{k}_2)\beta^*_{jn_2}(\mathbf{k}_2) = \langle n_i^f \rangle \langle n_j^f \rangle \ , \tag{A6a}$$

and (ii) gives

$$\frac{1}{N^2} \sum_{\mathbf{k}_1,n_1<\varepsilon_f} \beta_{in_1}(\mathbf{k}_1)\beta^*_{jn_1}(\mathbf{k}_1) e^{i\mathbf{k}_1\cdot\delta} \sum_{\mathbf{k}_2,n_2>\varepsilon_f} \beta_{jn_2}(\mathbf{k}_2)\beta^*_{in_2}(\mathbf{k}_2) e^{-i\mathbf{k}_2\cdot\delta} \ , \tag{A6b}$$

which is the correction to the mean-field term.

---

*Permanent address: The Department of Physics, University of Sheffield, Sheffield S3 7RH, United Kingdom.

†Present address: The Department of Physics, University of Illinois at Urbana-Champaign, Loomis Laboratory of Physics, 1110 West Green Street, Urbana, IL 61801.

[1]P. W. Anderson, Science **235**, 1196 (1987); F. C. Zhang and T. M. Rice, Phys. Rev. B **37**, 3759 (1988).

[2]K. A. Chao, J. Spalek, and A. M. Olès, J. Phys. C **10**, L271 (1977).

[3]S. Chakravarty, B. Halperin, and D. Nelson, Phys. Rev. B **39**, 2344 (1989); H. Q. Ding and M. S. Makivić, Phys. Rev. Lett. **64**, 1449 (1990).

[4]R. J. Birgeneau and G. Shirane, in *Physical Properties of High Temperature Superconductors,* edited by D. M. Ginsberg (World Scientific, Singapore, 1989).

[5]B. I. Shraiman and E. D. Siggia, Phys. Rev. Lett. **62**, 1564 (1989).

[6]C. L. Kane, P. A. Lee, T. K. Ng, B. Chakraborty, and N. Read, Phys. Rev. B **41**, 2653 (1990).

[7]I. Affleck and J. B. Marston, Phys. Rev. B **37**, 3774 (1988); P. Lederer, D. Poilblanc, and T. M. Rice, Phys. Rev. Lett. **63**, 1519 (1989); J. P. Rodriguez and B. Doucot (unpublished); S. Sachdev (unpublished).

[8]S. Liang and N. Trivedi, Phys. Rev. Lett. **64**, 232 (1990); D. Poilblanc, Y. Hasegawa, and T. M. Rice, Phys. Rev. B **41**, 1949 (1990); D. Poilblanc and Y. Hasegawa, *ibid.* **41**, 6899 (1990).

[9]See also, E. Fradkin and M. Stone, Phys. Rev. B **38**, 7215 (1988); R. Shankar, Phys. Rev. Lett. **63**, 203 (1989); P. A. Lee, *ibid.* **63**, 680 (1989).

[10]Y. Nagaoka, Phys. Rev. **147**, 392 (1966).

[11]Y. Hasegawa, P. Lederer, T. M. Rice, and P. B. Wiegmann, Phys. Rev. Lett. **63**, 907 (1989).

[12]Note that the $q=2$ phase with $\Phi_{av}=\pi$ gives the same spectrum as the uniform problem with one-half flux quantum per plaquette.

[13]X. G. Wen, F. Wilczek, and A. Zee, Phys. Rev. B **39**, 11 413 (1989).

[14]Recall that the π flux phases correspond to spin configurations in which spins on the A and B sublattices have polar angles α and $\beta=\pi-\alpha$, respectively. If $\alpha=\beta<\pi/2$ then $\Phi_p<\pi$.

[15]K. Kiefl *et al.*, Phys. Rev. Lett. **64**, 2082 (1990); K. Lyons *et al.*, *ibid.* **64**, 2949 (1990); S. Spielman *et al.*, *ibid.* **65**, 123 (1990).

[16]See, for example, D. C. Mattis, *The Theory of Magnetism I* (Springer-Verlag, Berlin, 1988), p. 252.